Revealing magnetic ground state of a layered cathode material by muon spin relaxation and neutron scattering experiments

Ping Miao, Rui Wang, Weiming Zhu, Jiajie Liu, Tongchao Liu, Jiangtao Hu, Shuankui Li, Zhijian Tan, Akihiro Koda, Fengfeng Zhu, Erxi Feng, Yixi Su, Takashi Kamiyama, Yinguo Xiao, and Feng Pan

View Online   Export Citation   CrossMark

ARTICLES YOU MAY BE INTERESTED IN

Revealing magnetic ground state of a layered cathode material by muon spin relaxation and neutron scattering experiments

Ping Miao,[1,2,a)] Rui Wang,[1,a)] Weiming Zhu,[1] Jiajie Liu,[1] Tongchao Liu,[1] Jiangtao Hu,[1] Shuankui Li,[1] Zhijian Tan,[2,3]
Akihiro Koda,[2,3] Fengfeng Zhu,[4] Erxi Feng,[4] Yixi Su,[4] Takashi Kamiyama,[2,3] Yinguo Xiao,[1,b)] and Feng Pan[1,b)]

AFFILIATIONS

[1] School of Advanced Materials, Peking University, Shenzhen Graduate School, Shenzhen 518055, China
[2] Institute of Materials Structure Science, High Energy Accelerator Research Organization (KEK), Tokai, Ibaraki 319-1106, Japan
[3] Department of Materials Structure Science, Sokendai (The Graduate University for Advanced Studies), Tokai, Ibaraki 319-1106, Japan
[4] Jülich Centre for Neutron Science, Forschungszentrum Jülich GmbH, Outstation at MLZ, D-85747 Garching, Germany

[a)] Contributions: P. Miao and R. Wang contributed equally to this work.
[b)] Electronic addresses: xiaoyg@pkusz.edu.cn and panfeng@pkusz.edu.cn.

ABSTRACT

Although the majority of studies on battery materials have focused on enhancing their electrochemical performance, the understanding of their magnetic and atomic structures as well as the intimate connections between these structures and properties is significant. Muon spin relaxation (μSR) spectroscopy and neutron scattering techniques at low temperature have been used to explore the nature of the magnetic state of $Li(Ni_{0.4}Mn_{0.4}Co_{0.2})O_2$ cathode materials. Interestingly, the μSR experiment reveals that the spins of Ni/Mn/Co ions turn glassy at a low temperature of 19 K, while the unprecedented spin dynamics survives until the base temperature of 5.6 K. Moreover, the complementary neutron scattering measurements show magnetic diffuse scattering signals in the form of a broad peak at $Q = 1.6$ Å^{-1} attributed to short-range spin correlation which establishes below $\sim$120 K. Upon cooling to as low as 480 mK, long-range magnetic order still could not be established. The inelastic neutron scattering intensities demonstrate clearly the existence of dynamic spin fluctuations. In contrast to the conventional spin glass system, the coexistence of both dynamic and static components in the ground state suggests an unconventional spin glass state in magnetically frustrated $Li(Ni_{0.4}Mn_{0.4}Co_{0.2})O_2$ cathode materials for Li-ion batteries.

Lithium-ion batteries (LIBs) have been widely used in mobile electronic devices and have been recently playing the lead role in power electric vehicles.[1–4] Among the well-known cathode materials, layered lithium transition metal oxides (TMOs) $LiNi_xMn_yCo_zO_2$ (NMC, $x + y + z = 1$) are considered promising candidates owing to their two-dimensional ion-channel and high-energy density. The high performance of NMC can be attributed to the synergistic effect of the three individual transition metals (TMs) since each individual TM can strengthen the performance of NMC materials in certain aspects.[5–11]

Despite the fact that numerous research activities on NMC aim at improving their electrochemical performance, some basic physical properties such as magnetism in NMC are overlooked. Given that the transition metal ions in NMC play a dominant role in determining the

energy density of layered cathode materials and they are all magnetic in nature, it is of particular interest to explore the magnetism in NMC.[12,13] Moreover, in our previous work on the relationship between structures and properties of NMC materials, it was found that the magnetic frustration and superexchange interaction play an important role in tuning the Li/Ni exchange ratio in layered NMC materials.[14,15]

All NMC compounds are isostructural and crystallized in the rhombohedral structure with space group *R-3m* in an ambient environment, as illustrated in Fig. 1(a). The alternating planes of Li and TM oxide slabs built up of edge-sharing octahedra in NMC and TM spins form a two-dimensional triangular lattice [Fig. 1(b)]. As it is not possible to minimize the interaction energy simultaneously for all pairs of nearest-neighbor spins in the magnetic triangular lattice, the
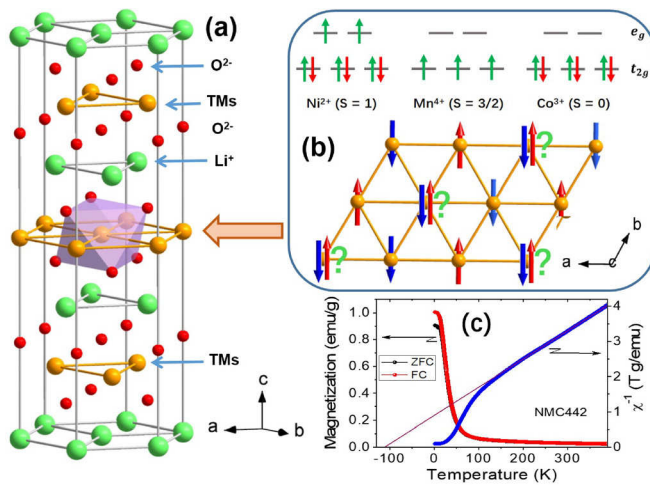
FIG. 1. (a) Schematic view of the crystal structure of NMC cathode materials. (b) Spin states of TM ions and top view of the frustrated triangular layer of TMs. (c) Temperature dependence of the magnetization and inverse magnetic susceptibility χ^{-1} of NMC442 measured in the zero-field-cooling (ZFC) and field-cooling (FC) mode under a magnetic field of 1000 Oe. The solid straight line indicates the Curie-Weiss fit to inverse susceptibility in the high temperature region from 200 to 390 K as described in the text.

manifolds of possible ground states in the two-dimensional triangular lattice could be established, leading to the frustration of the whole system and resulting in an exotic ground state. Many special ground states have been proposed to describe the magnetic ground states of the frustrated system, such as spin liquid, spin ice, two-dimensional Ising ferromagnets, or magnetic Coulomb phases.[16–19] For instance, it was found that the ground state structure of $LiNiO_2$ is not homogeneous and the unconventional magnetism observed in $LiNiO_2$ may be explained in the context of the interplay between Ni^{3+} $3d$ orbitals, trimer units, and domains under a triangular symmetry.[20] As for the $LiCoO_2$ counterpart, perfectly stoichiometric $LiCoO_2$ will show no local moment because its Co^{3+} is in a low-spin d_6, whereas the material will show a magnetic moment if a nonstoichiometric amount of Li is incorporated.[21] Nevertheless, the nature of the magnetic state and spin correlation in the NMC system is still under debate and has not yet been understood in spite of the extensive research work.

Figure 1(c) shows the temperature dependence of the magnetization of NMC442 under a magnetic field of 1000 Oe. With decreasing temperature, the magnetizations obtained from both zero-field-cooling (ZFC) and field-cooling (FC) modes increase gradually from 390 to 120 since the sample is still in the high temperature paramagnetic state, while the magnetization increases rapidly below 120 K because of the formation of magnetic correlations and static moments. It is also observed that the ZFC and FC curves start bifurcating at around 19 K, indicating the existence of a severe history dependence, which is a characteristic feature of the spin glass system. The temperature dependence of the inverse susceptibility χ^{-1} of NMC442 is also exhibited in Fig. 1(c). It is known that the magnetic susceptibility of localized noninteracting magnetic ions in the high temperature region can be written as: $\chi(t) = C/(T - \Theta_{CW})$. The susceptibility strictly follows the Curie-Weiss behavior above 200 K, while the inverse susceptibility χ^{-1} deviated from the Curie-Weiss estimation below 120 K, indicating

the onset of considerable magnetic correlations. The effective paramagnetic moment is deduced to be 3.09 μ_B/f.u. and the Curie-Weiss temperature is -96.2 K, indicating that the dominant magnetic interactions are antiferromagnetic in NMC442.

The zero-field muon spin relaxation (μSR) spectra contain significant contributions from relaxations induced by the nuclear dipolar field. By applying a weak longitudinal magnetic field (LF) of 100 Oe, we could eliminate the effect of the nuclear dipolar field without disturbing the relaxations from the magnetic field of Ni/Mn/Co spins [see Fig. S1(a) in the supplementary material]. The observed initial asymmetry (corrected asymmetry at $t = 0$) of spectra of 100 Oe as shown in Fig. 2(a), the same as that of zero-field μSR spectra, abruptly decreases upon cooling at low temperatures, indicating that the relaxation rate of the spectra rises beyond the time resolution of the pulsed muon source. The sudden increase in the relaxation rate generally arises from the critical slowing down of magnetic moments, i.e., the
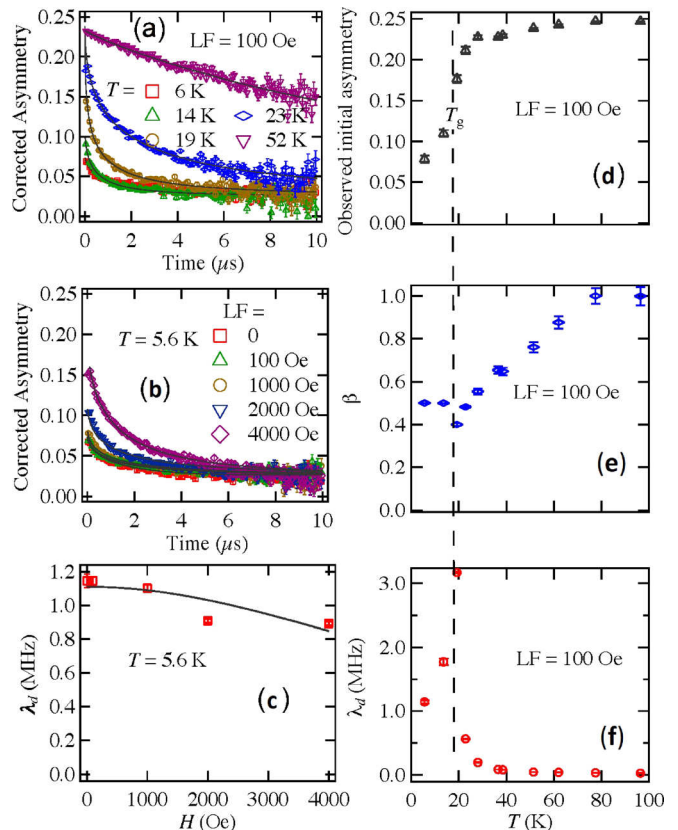
FIG. 2. Muon spin relaxation (μSR) measurements of Li(Ni$_{0.4}$Mn$_{0.4}$Co$_{0.2}$)O$_2$. (a) μSR spectra under a longitudinal field (LF) of 100 Oe at various temperatures. The observed initial asymmetry (corrected asymmetry at $t = 0$) does not vary upon changing LF from the zero-field to 100 Oe. (b) μSR spectra at 5.6 K under various LFs. (c) Muon spin depolarization rate λ_d as a function of LF. (d) Observed initial asymmetry as a function of temperature obtained from the spectra under LF $= 100$ Oe. (e) Index β as a function of temperature obtained from fitting the spectra under LF $= 100$ Oe to Eq. (2) (above T_g). β was fixed to $1/2$ in the analysis below T_g. (f) Muon spin depolarization rate λ_d as a function of temperature obtained fitting the spectra under LF $= 100$ Oe to Eq. (2) (above T_g) and Eq. (4) (below T_g). The solid lines are the fits to Eq. (4).

formation of static moments. Corroborating evidence for the static moments comes from the increase in the observed initial asymmetry upon applying LFs at 5.6 K [see Fig. 2(b)]. The temperature dependence of the observed initial asymmetry [Figs. 2(d) and S1(b) in the supplementary material] suggests that the static components initiate at about 19 K with decreasing temperatures.

To understand the nature of this static component, we performed quantitative analysis using "musrfit"[22] on the spectra with various models. As shown in Fig. S1(c) in the supplementary material, the spectra close to (above) 19 K cannot be fitted to a simple exponential function

$$A_S G_Z(t) = A_d \, exp(-\lambda_d t) + A_{bg}, \tag{1}$$

where A_s denotes the intrinsic initial muon-decay asymmetry, A_d the initial asymmetry of the exponential term, and A_{bg} the background, $A_d + A_{bg} = A_s$. The constant background A_{bg}, extracted from zero-field spectra at 5.6 K, was applied in fitting at all temperatures and LFs hereafter. $G_z(t)$ represents the polarization of muon spins in the sample. The parameter λ_d is the dynamic depolarization rate (relaxation rate), and the corresponding exponential term describes typical dynamic spin fluctuations above magnetic ordering temperature. Instead, we found that the spectra can be characterized by a stretched-exponential function

$$A_S G_Z(t) = A_d \, exp\left[(-\lambda_d t)^\beta\right] + A_{bg}. \tag{2}$$

As shown in Fig. 2(e), the obtained index β decreases from 1 (simple exponential function) to 1/2 when approaching 19 K upon cooling, suggesting that the spin dynamics cannot be characterized by a single spin correlation time τ, i.e., the spins turn glassy at low temperatures. According to the spin glass model,[23,24] the β value is predicted to be 1/2, which is consistent with our observations. Therefore, the characteristic temperature 19 K should be defined as the freezing temperature T_g of spin glass.

Below T_g, in addition to the static magnetic moment, unprecedented spin dynamics was observed down to the base temperature of 5.6 K. As shown in Fig. 2(b), by applying LF of 4000 Oe at 5.6 K, the static component of spin glass is fully polarized parallel to the muon spin orientation so that the remaining damping of the spectra unambiguously indicates the dynamic spin fluctuations. For the coexistence of static and dynamic components of spin glass, the zero-field (or weak LF) μSR spectra are generally described by the following function:[23,24]

$$A_S G_Z(t) = \frac{1}{3} A_{slow} \, exp\left[(-\lambda_d t)^{\frac{1}{2}}\right] + \frac{2}{3} A_{fast} \left[1 - \frac{a_s^2 t^2}{\left(\lambda_d t + a_s^2 t^2\right)^{\frac{1}{2}}}\right]$$
$$\times \, exp\left[(-\lambda_d t)^{\frac{1}{2}}\right] + A_{bg}, \tag{3}$$

where a_s and λ_d correspond to the static and dynamic components, respectively. Equation (3) consists of a slow relaxation term (1/3 term) and a fast relaxation term (2/3 term). In our μSR experiment, the fast relaxation term manifests itself as the decrease in the observed initial asymmetry below T_g due to the limitation of time resolution so that only the slow relaxation term as shown in Eq. (4) is needed to describe the μSR spectra under LF of 100 Oe

$$A_S G_Z(t) = \frac{1}{3} A_{slow} \, exp\left[(-\lambda_d t)^{\frac{1}{2}}\right] + A_{bg}. \tag{4}$$

The dynamic depolarization rate λ_d obtained from fitting to Eq. (2) (above T_g) and Eq. (4) (below T_g) is plotted in Fig. 2(f), which shows a distinctly unusual temperature dependence below T_g with respect to conventional spin glass systems.[23–25] Specifically, the λ_d value of typical spin glass systems decays steeply to zero (or close to zero) upon cooling down to $\sim 0.5\,T_g$ whereas the λ_d value of $Li(Ni_x Mn_y Co_z)O_2$ remains over 1 MHz at base temperature (below $0.5\,T_g$), indicating the anomalous strong spin fluctuations in the ground state of NMC442.

As show in Fig. 2(b), the μSR spectra under stronger LFs at base temperature were also fitted to Eq. (4) since the effect of LFs on the fast damping term only presents in terms of the increase in the observed initial asymmetry and can be accounted by A_{slow}. According to the Redfield theory, the field dependence of λ_d is formulated as follows:

$$\lambda_d = \frac{4 a_d^2 \nu}{\nu^2 + \left(\gamma_\mu H\right)^2}, \tag{5}$$

where γ_μ is the muon gyromagnetic ratio ($2\pi \times 0.01355342$ MHz/Oe), H the longitudinal magnetic field, ν the spin fluctuation rate (the reciprocal of spin correlation time τ), and $a_d = \sqrt{1 - Q}a$ with Q being the Edward-Anderson order parameter ($Q = 0$ above T_g) and a the average amplitude of the magnetic field. The fitting to Eq. (5) as shown in Fig. 2(c) gives $\nu = 6(1) \times 10^8$ Hz and $A_d = 1.3(1) \times 10^7$ Hz at base temperature.

As a special magnetic phenomenon, spin glass behavior can be considered as an intrinsic effect of competition of magnetic interactions. Thus, neutron scattering measurements could further contribute to our understanding of spin glass behavior since it can assert not only static magnetic order but also spin excitations. Different from the μSR technique, which broadly averages over all momentum space, neutron scattering possesses the ability to probe the signal for various wave vectors. Thus, the polarized neutron scattering measurements were carried out on the NMC442 powder sample, and the details of the experimental methodology are provided in the supplementary material.

In contrast to the nuclear coherent scattering pattern (see Fig. S2 in the supplementary material), the magnetic signal did not exhibit any sharp reflection instead of the broad magnetic diffuse scattering peak, as shown in Fig. 3(a). The absence of the prominent magnetic peak indicates that long-range magnetic order does not exist with temperature as low as 480 mK. Nevertheless, strong magnetic diffuse scattering is revealed in NMC442 even down to the base temperature. The evolution of the integrated intensity of the magnetic diffuse scattering signal at various temperatures is plotted in Fig. 3(b). Clear magnetic diffuse scattering has emerged in the large temperature range from the base temperature to around 90 K, and they can be described properly by a Lorentzian function. Moreover, it is located at the position of $Q = 1.6$ Å^{-1} and most pronounced at around $T_g = 19$ K. Although the diffuse peak becomes subdued upon further cooling from T_g, the prominent signal demonstrates that the spin motion is still not yet frozen. As shown in Fig. 3(c), the full-width-half-maximum (FWHM) exhibits a similar trend to integrated intensity. Generally, the inverse full-width at half-maximum (FWHM) of the broad magnetic diffuse scattering peak can be taken as a measure of the spin correlation length (ξ),[26] i.e., $\xi = 2\pi/$FWHM. At the base temperature of 480 mK, the FWHM is about 0.9 Å^{-1} and the correlation length is estimated to be
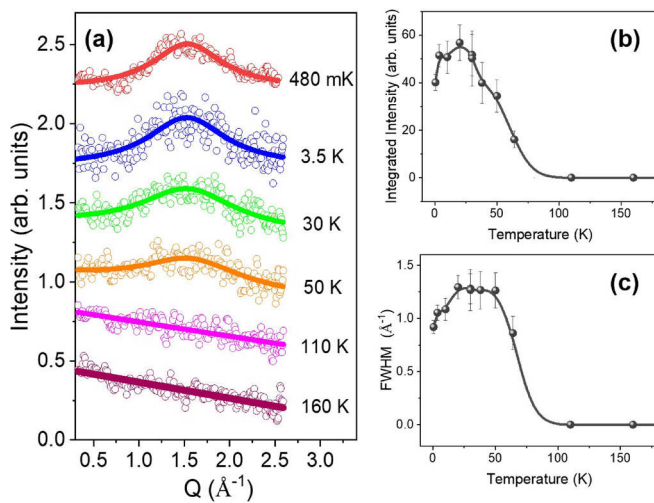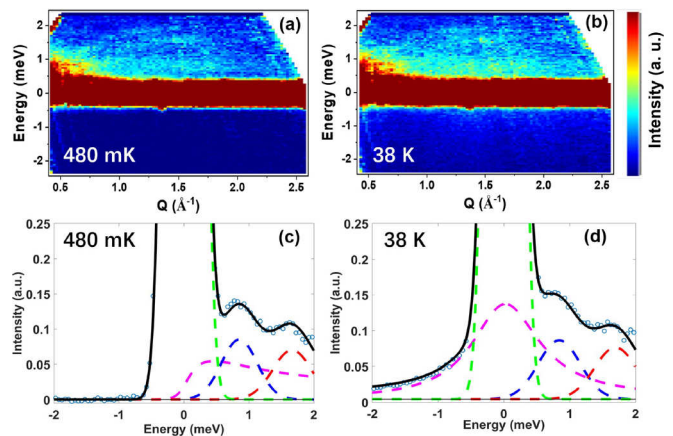
FIG. 3. Polarized neutron diffraction pattern for NMC442 at different temperatures. (a) Magnetic diffuse scattering signals are observed well above T_g and disappear at T_s, indicating strong spin correlations. The integrated intensities (b) and FWHM (c) as a function of temperature can be deduced by fitting the diffused neutron scattering signal by a simple Lorentzian.

FIG. 4. Inelastic neutron scattering signal is observed at 480 mK (a) and 38 K (b), exhibiting strong dynamic components of the spin glass state. (c) and (d) The dynamic structure factor $S(Q, \omega)$ emanating from $Q = 0.6$–$2.0\,\text{Å}^{-1}$ of NMC442 at 480 mK (c) and 38 K (d). The quasi-elastic components are indicated by magenta dashed-lines. The red and blue dashed-lines denote the inelastic components from spin excitations. The green dashed-lines correspond to the instrumental resolution. The black solid lines represent the sum of both quasi-elastic and inelastic components.

about 6.98 Å. The diffuse scattering signal in NMC442 is most likely due to the short-range order that originates from the exchange coupling and magnetic frustration in the triangular lattice of TM planes.

As a powerful spectroscopic technique, inelastic neutron scattering can be used for probing the collective spin excitations in a magnetic system. Spin dynamics properties such as magnetic correlations can be obtained from the neutron dynamic structure factor as a function of both energy and momentum transfers, over the reciprocal space. Figures 4(a) and 4(b) show the Bose-factor-corrected $S(Q, \omega)$ plots for NMC442 at temperatures of 480 mK and 38 K. The strip around zero energy transfer is mainly attributed to nuclear Bragg reflections, while the magnetic scattering intensities distributed over the negative and positive sides of the energy transfer correspond to the dynamic structure factors of neutron energy gain and energy loss processes, respectively. As shown in Fig. 4(a), the magnetic excitation contribution at 480 mK is mainly located at the energy loss side of the neutron spectra (positive energies), whereas the quasi-elastic component increases significantly as shown in Fig. 4(b).

In order to analyze the magnetic components of the dynamic structure factor $S(Q, \omega)$ in detail, we have examined the line shape of $S(Q, \omega)$ for constant Q values. The energy cuts of $S(Q, \omega)$ at 480 mK and 38 K are plotted in Figs. 4(c) and 4(d), respectively. The central elastic peak is fitted with a single Gaussian function, whose width corresponds to the instrumental resolution. As shown in Fig. 4(c), the line shape of $S(Q, \omega)$ at 480 mK can be properly fitted by one Lorentzian shaped quasi-elastic peak nearby the elastic line (as described in the experimental methodology in the supplementary material), together with two Gaussian peaks located at the neutron energy loss side. Upon heating to 38 K, the quasi-elastic scattering dominates the $S(Q, \omega)$ profile. The magnetic correlations persist and thereby also lead to an inelastic response. Figure 4(d) presents the best fit results obtained by using both quasi-elastic and inelastic components for the measured data at 38 K. These two inelastic neutron scattering components with a

Gaussian peak shape are due to spurious scattering as they do not show any temperature dependence. The quasi-elastic intensity can be described by a single Lorentzian with its width determined by thermal fluctuations. According to the fitting results, the width Γ decreases from 0.62 meV at 38 K to 0.12 meV at 480 mK, indicating a remarkable slowing down of the spin fluctuations. Nevertheless, the existence of the quasi-elastic neutron scattering signal at both 480 mK and 38 K reveals robust dynamic components of the spin glass state.

Generally, a collective freezing of individual spin motion accompanied by no periodic long-range order occurs at low temperature in the spin glass system.[27–29] Actually, the spin glass state of NMC442 has been proposed and identified by performing frequency dependences of the ac magnetic susceptibilities.[30,31] However, although these studies have probed spin glass transitions, they have not elucidated the remnant dynamic components in the magnetic ground state of NMC442. In the present work, it was found that the dynamic spin fluctuations persist even at low temperature in NMC442 although the spins of transition metals turn glassy at low temperature, which differs from traditional spin glass behavior, suggesting an unconventional spin glass state. It is fair to presume that the strong magnetic frustration is the main driving force for the emergence of the unconventional spin glass phase in NMC442. The observed unconventional spin glass state might be related to topological glassy states as revived recently, i.e., a spin jam state induced by quantum fluctuations in the strongly frustrated system.[29,32] Nevertheless, although our study has revealed the unconventional spin glass phase in the layered cathode material, a further theoretical study of the formation of this unconventional spin glass state would clearly be of future interest.

See the supplementary material for more experimental details, device characterization, and the numerical value of all the parameters determined in this work.

REFERENCES

[1]M. S. Whittingham, Chem. Rev. **35**, 4271 (2004).

[2]M. Armand and J. M. Tarascon, Nature **451**, 652 (2008).

[3]J. Lu, Z. Chen, Z. Ma, F. Pan, L. A. Curtiss, and K. Amine, Nat. Nanotechnol. **11**, 1031 (2016).

[4]J. B. Goodenough and Y. Kim, Chem. Mater. **22**, 587 (2010).

[5]Z. Liu, A. Yu, and J. Y. Lee, J. Power Sources **81–82**, 416 (1999).

[6]Y. Wei, J. Zheng, S. Cui, X. Song, Y. Su, W. Deng, Z. Wu, X. Wang, W. Wang, M. Rao et al., J. Am. Chem. Soc. **137**, 8364 (2015).

[7]A. Manthiram, Y. You, H. Celio, A. Dolocan, and J. Li, Angew. Chem., Int. Ed. **57**, 6480 (2018).

[8]J. X. Zheng, T. C. Liu, Z. X. Hu, Y. Wei, X. H. Song, Y. Ren, W. D. Wang, M. M. Rao, Y. Lin, Z. H. Chen et al., J. Am. Chem. Soc. **138**, 13326 (2016).

[9]H. J. Noh, S. Youn, S. Y. Chong, and Y. K. Sun, J. Power Sources **233**, 121 (2013).

[10]W. Li, X. Liu, H. Celio, P. Smith, A. Dolocan, M. Chi, and A. Manthiram, Adv. Energy Mater. **8**, 1703154 (2018).

[11]H. G. Kim, S. T. Myung, J. K. Lee, and Y. K. Sun, J. Power Sources **196**, 6710 (2011).

[12]N. A. Chernova, G. M. Nolis, F. O. Omenya, H. Zhou, Z. Li, and M. S. Whittingham, J. Mater. Chem. **42**, 9865 (2011).

[13]C. M. Julien, A. Ait-Salah, A. Mauger, and F. Gendron, Ionics **12**, 21 (2006).

[14]J. Zheng, G. Teng, C. Xin, Z. Zhuo, J. Liu, Q. Li, Z. Hu, M. Xu, S. Yan, W. Yang et al., J. Phys. Chem. Lett. **8**, 5537 (2017).

[15]Y. Xiao, T. Liu, J. Liu, L. He, J. Chen, J. Zhang, P. Luo, H. Lu, R. Wang, and W. Zhu, Nano Energy **49**, 77 (2018).

[16]A. P. Ramirez, Nature **421**, 483 (2003).

[17]S. T. Bramwell and M. J. Gingras, Science **294**, 1495 (2002).

[18]Y. Han, Y. Shokef, A. M. Alsayed, P. Yunker, T. C. Lubensky, and A. G. Yodh, Nature **456**, 898 (2008).

[19]M. J. Gingras, Science **326**, 375 (2009).

[20]J. H. Chung, T. Proffen, S. Shamoto, A. M. Ghorayeb, L. Croguennec, W. Tian, B. C. Sales, R. Jin, D. Mandrus, and T. Egami, Phys. Rev. B **71**, 4410 (2005).

[21]J. T. Hertz, Q. Huang, T. Mcqueen, T. Klimczuk, J. W. G. Bos, L. Viciu, and R. J. Cava, Phys. Rev. B **77**, 5119 (2008).

[22]A. Suter and B. M. Wojek, Phys. Procedia **30**, 69 (2012).

[23]Y. J. Uemura, T. Yamazaki, D. R. Harshman, M. Senba, and E. J. Ansaldo, Phys. Rev. B **31**, 546 (1985).

[24]R. H. Heffner, L. P. Le, M. F. Hundley, J. J. Neumeier, G. M. Luke, K. Kojima, B. Nachumi, Y. J. Uemura, D. E. Maclaughlin, and S. W. Cheong, Phys. Rev. Lett. **77**, 1869 (1996).

[25]C. Boekema, V. A. M. Brabers, R. L. Lichti, A. B. Denison, D. W. Cooke, R. H. Heffner, R. L. Hutson, M. E. Schillaci, D. E. Maclaughlin, and S. A. Dodds, Hyperfine Interact. **31**, 369 (1986).

[26]H. F. Li, C. Zhang, A. Senyshyn, A. Wildes, K. Schmalzl, W. Schmidt, M. Boehm, E. Ressouche, B. Hou, P. Meuffels et al., Front. Phys. **2**, 42 (2014).

[27]J. A. Mydosh, Spin Glasses: An Experimental Introduction (Taylor & Francis, London, 1993).

[28]Z. Ma, J. Wang, Z. Y. Dong, J. Zhang, S. Li, S. H. Zheng, Y. Yu, W. Wang, L. Che, and K. Ran, Phys. Rev. Lett. **120**, 087201 (2018).

[29]I. Klich, S. H. Lee, and K. Iida, Nat. Commun. **5**, 3497 (2014).

[30]F. Du, X. Bie, Y. Chen, Y. Wei, L. Liu, C. Wang, G. Zou, and G. Chen, J. Appl. Phys. **106**, 053904 (2009).

[31]N. A. Chernova, M. Ma, J. Xiao, M. S. Whittingham, J. Breger, and C. P. Grey, Chem. Mater. **19**, 4682 (2007).

[32]J. J. Yang, A. Samarakoon, S. Dissanayake, H. Ueda, I. Klich, K. Iida, D. Pajerowski, N. P. Butch, Q. Huang, J. R. D. Copley et al., Proc. Natl. Acad. Sci. U. S. A. **112**, 11519 (2015).